Int. J. Heat Mass Transfer. Vol. 28, No. 2, pp. 467–477, 1985
Printed in Great Britain

0017-9310/85 $3.00 + 0.00
Pergamon Press Ltd.

Natural convection heat transfer below downward facing horizontal surfaces*

T. SCHULENBERG†

Kernforschungszentrum Karlsruhe, Institut für Reaktorbauelemente, Postfach 3640, 7500 Karlsruhe 1, F.R.G.

(*Received* 19 *March* 1984)

Abstract—The laminar steady-state convection below a horizontal infinite strip and below a horizontal circular plate is determined analytically for the limiting case of high Prandtl numbers. The plate surface is assumed to be either isothermal or uniformly heated. This convection is caused by the non-uniform temperature distribution at the edges of the plate. Therefore, this problem has to be described by an elliptic differential equation which was not taken into account in earlier integral methods. Applying the method of matched asymptotic expansions, similarity solutions are deduced for a region around the stagnation point. Moreover, an interpolation with the limiting case of low Prandtl numbers yields heat transfer correlations for arbitrary Prandtl numbers.

INTRODUCTION

NATURAL convection below downward facing horizontal surfaces differs fundamentally from convection at inclined plates. There, or even on upwards facing horizontal plates, heat transfer is a function of the distance from the leading edge of the plate. The flow is driven by the local buoyancy force within the boundary layer. It can be determined with the boundary layer equations neglecting any outer flow field. This problem is parabolic.

In contrast to inclined plates, local heat transfer below a horizontal flat plate is a function of the total plate length. As the temperature distribution is stable below an infinite plate, this convection is caused by the singular behaviour of velocity and temperature at the edges. The flow is directed from a stagnation point at the plate centre towards the edges. The accelerating force which acts upstream from the edges can be described only by an elliptic differential equation. This means that the flow outside the boundary layer must be included, although it is small, if the heat transfer at any point of the plate is to be evaluated properly. In this case current solution procedures fail because the outer flow itself will be driven by the buoyancy forces inside the boundary layer.

A great number of theoretical approaches were published, in which an attempt was made to circumvent this problem. Applying an integral method to the boundary layer equations, the finite size of the plate was included by an artificial boundary condition for the boundary layer thickness δ at the edges. Singh *et al.* [1] assumed that δ tends towards zero at the edges, Singh and Birkebak [2] assumed that the horizontal derivative of δ tends towards infinity there, Fujii *et al.* [3] and Clifton and Chapman [4] tried to obtain a critical thickness of δ and Hatfield and Edwards [5] added an empirical extrapolation length to the total length of the plate to interpolate their data. All these efforts neglected the important role of the outer flow. Moreover, integral methods were based on empirical boundary layer profiles which had been measured in air but applied to arbitrary Prandtl numbers. These results are only reasonable in the range of the experimental data. Extrapolations to higher or lower Prandtl numbers, applications to non-isothermal plates or to higher Rayleigh numbers etc. are thus doubtful.

The method of matched asymptotic expansions has been proposed by Schulenberg [6] in order to include the elliptic behaviour of this convection. For a special application to liquid metals, this procedure was limited to low Prandtl numbers. A potential flow around the plate with an unknown upstream velocity was taken as the outer expansion, and a temperature boundary layer as the inner expansion. Both expansions were matched with an energy balance in the vicinity of the stagnation point. This matching correlated the unknown upstream velocity of the outer flow with the Grashof number and the Prandtl number. The main result was that local similarity solutions were obtained for the temperature boundary layer.

A similar procedure is applied here to determine the convective flow for high Prandtl numbers. In this case, viscosity forces dominate within the temperature boundary layer. Therefore the outer expansion is described as a Stokes' flow instead, which again is a solution to an elliptic problem. Both asymptotes of low and high Prandtl numbers are then interpolated to yield a general expression for heat transfer for arbitrary Prandtl numbers.

Similarity solutions for high Prandtl numbers

For the limiting case of high Prandtl numbers, the laminar steady-state convection below a horizontal

*This work is part of a Ph.D. thesis, University of Karlsruhe, 1984.

† Present address: Dornier System GmbH, Postfach 1360, D-7990 Friedrichshafen, F.R.G.

NOMENCLATURE

A — $Pe^{5/4}/(Gr\,Pr)$ for specified surface temperature; $Pe^{3/2}/(Gr^*Pr)$ for specified surface heat flux
e — exponent for interpolation
g — acceleration due to gravity
Gr — Grashof number, $\alpha g(T_w - T_\infty)R^3/\nu^2$
Gr^* — modified Grashof number, $\alpha g q_w R^4/(\lambda \nu^2)$
m — $m = n-1$
M — dimensionless stream function, $\psi/(v_\infty R)$
n — $n = 0$ for two-dimensional convection; $n = 1$ for axisymmetric convection
Nu — local Nusselt number near the stagnation point $q_w R/(\lambda(T_w - T_\infty))$
$\overline{Nu}$ — mean Nusselt number
Nu_1 — Nusselt number averaged over a plate length
p — pressure
Pe — Peclet number, $v_\infty R/\kappa$
Pr — Prandtl number ν/κ
q_w — surface heat flux
r — horizontal coordinate
R — half-width of the infinite strip or radius of the circular plate
Ra — Rayleigh number, $Gr\,Pr$
Ra^* — modified Rayleigh number, Gr^*Pr
T — temperature
T_w, T_∞ — surface temperature and ambient temperature, respectively
u — horizontal velocity component
U — profile of the horizontal velocity, $\int_0^\eta \omega_1 d\eta$
v — vertical velocity component
v_∞ — upstream velocity (unknown)
V — profile of the vertical velocity, $\int_0^\eta U d\eta$
x_1, x_2 — elliptic coordinates
z — vertical coordinate.

Greek symbols

α — thermal expansion coefficient
η — dimensionless vertical coordinate, $Pe^{1/4}z/R$
θ — dimensionless temperature; $\theta = (T - T_\infty)/(T_w - T_\infty)$ for specified surface temperature; $\theta = Pe^{1/4}\lambda(T - T_\infty)/(q_w R)$ for specified surface heat flux
θ_0, θ_1 — coefficients of the temperature power series expansion
λ — thermal conductivity
κ — thermal diffusivity
ν — kinematic viscosity
ξ — dimensionless horizontal coordinate, r/R
ρ — density
σ — positive root of equation (18)
ϕ — potential
ψ — stream function
ω — dimensionless vorticity, $R^2 A\Omega/(\kappa\, Pe^{3/4})$
ω_1 — profile of the vorticity, $\omega^I/(2\xi)$
Ω — vorticity.

Superscripts

I — iterated function.

infinite strip and below a horizontal circular plate will be determined. Typical streamlines and temperature profiles are sketched in Fig. 1. The plate surface is assumed to be isothermal or uniformly heated.

Using the Boussinesq approximation, but without applying boundary layer approximations, the governing equations are

$$\frac{\partial u}{\partial r} + n\frac{u}{r} + \frac{\partial v}{\partial z} = 0, \tag{1}$$

$$u\frac{\partial u}{\partial r} + v\frac{\partial u}{\partial z} = -\frac{1}{\rho}\frac{\partial p}{\partial r} + \nu\left(\frac{\partial^2 u}{\partial r^2} + n\frac{\partial}{\partial r}\left(\frac{u}{r}\right) + \frac{\partial^2 u}{\partial z^2}\right), \tag{2}$$

$$u\frac{\partial v}{\partial r} + v\frac{\partial v}{\partial z} = -\frac{1}{\rho}\frac{\partial p}{\partial z} + \nu\left(\frac{\partial^2 v}{\partial r^2} + n\frac{1}{r}\frac{\partial v}{\partial r} + \frac{\partial^2 v}{\partial z^2}\right) - \alpha g(T - T_\infty), \tag{3}$$

$$u\frac{\partial T}{\partial r} + v\frac{\partial T}{\partial z} = \kappa\left(\frac{\partial^2 T}{\partial r^2} + n\frac{1}{r}\frac{\partial T}{\partial r} + \frac{\partial^2 T}{\partial z^2}\right), \tag{4}$$

where $n = 0$ for a two-dimensional convection below an infinite strip, and $n = 1$ for an axisymmetric convection below a circular plate.

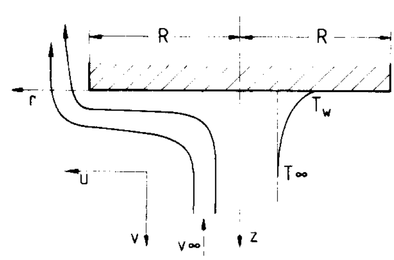

FIG. 1. Coordinate system and sketch of the streamlines.

The continuity equation, equation (1), can be satisfied by introducing a stream function ψ, with

$$u = \frac{\partial \psi}{\partial z}, \quad v = -\frac{\partial \psi}{\partial r} - n\frac{\psi}{r}. \tag{5}$$

Moreover, a vorticity, Ω, is introduced as

$$\Omega = \frac{\partial u}{\partial z} - \frac{\partial v}{\partial r}. \tag{6}$$

The number of free parameters is reduced by a transformation to the following dimensionless quantities:

$$\xi = \frac{r}{R}, \quad \eta = \frac{z}{R}Pe^{1/4},$$

$$M = \frac{\psi}{v_\infty R}, \quad \omega = \frac{R^2}{\kappa}\frac{A}{Pe^{3/4}}\Omega,$$

$$Pe = \frac{v_\infty R}{\kappa}, \quad Pr = \frac{\nu}{\kappa}$$

and

$$\theta = \frac{T - T_\infty}{T_w - T_\infty}, \quad A = \frac{Pe^{5/4}}{Gr\,Pr}, \quad Gr = \frac{\alpha g(T_w - T_\infty)R^3}{\nu^2} \tag{7}$$

for a specified surface temperature, or

$$\theta = Pe^{1/4}\frac{(T - T_\infty)}{q_w R}, \quad A = \frac{Pe^{3/2}}{Gr^* Pr}, \quad Gr^* = \frac{\alpha g q_w R^4}{\lambda \nu^2} \tag{8}$$

for a specified surface heat flux.

In analogy to the asymptote of low Prandtl numbers derived in [6], a Peclet number, Pe, containing an unknown velocity, v_∞, far below the plate, is treated as a separate variable in this representation. As this upstream velocity is driven by the buoyancy forces close to the plate, this Peclet number is related to the Grashof number, Gr or Gr^*, and to the Prandtl number, Pr. It is the aim of the iterative procedure described here, to determine this relation.

In a dimensionless form, the governing equations (1) to (4) can be written as

$$\frac{1}{Pe^{1/2}}\left[\frac{\partial^2 M}{\partial \xi^2} + n\frac{\partial}{\partial \xi}\left(\frac{M}{\xi}\right)\right] + \frac{\partial^2 M}{\partial \eta^2} = \frac{\omega}{A\,Pe^{3/4}}, \tag{9}$$

$$\frac{Pe^{3/4}}{Pr}\left[\frac{\partial M}{\partial \eta}\left(\frac{\partial \omega}{\partial \xi} - n\frac{\omega}{\xi}\right) - \left(\frac{\partial M}{\partial \xi} + n\frac{M}{\xi}\right)\frac{\partial \omega}{\partial \eta}\right]$$
$$= \frac{1}{Pe^{1/2}}\left[\frac{\partial^2 \omega}{\partial \xi^2} + n\frac{\partial}{\partial \xi}\left(\frac{\omega}{\xi}\right)\right] + \frac{\partial^2 \omega}{\partial \eta^2} + \frac{\partial \theta}{\partial \xi}, \tag{10}$$

$$\frac{\partial M}{\partial \eta}\frac{\partial \theta}{\partial \xi} - \left(\frac{\partial M}{\partial \xi} + n\frac{M}{\xi}\right)\frac{\partial \theta}{\partial \eta}$$
$$= \frac{1}{Pe^{3/4}}\left[\frac{1}{Pe^{1/2}}\left(\frac{\partial^2 \theta}{\partial \xi^2} + n\frac{1}{\xi}\frac{\partial \theta}{\partial \xi}\right) + \frac{\partial^2 \theta}{\partial \eta^2}\right]. \tag{11}$$

The inertial terms of the vorticity transport equation, equation (10), can be cancelled within the limit of high Prandtl numbers which will be treated here exclusively. Neglecting terms with $1/Pr$ one obtains instead of equation (10), the simplified equation:

$$\frac{1}{Pe^{1/2}}\left[\frac{\partial^2 \omega}{\partial \xi^2} + n\frac{\partial}{\partial \xi}\left(\frac{\omega}{\xi}\right)\right] + \frac{\partial^2 \omega}{\partial \eta^2} = -\frac{\partial \theta}{\partial \xi}. \tag{12}$$

For high Peclet numbers, fluid motion can be divided into a temperature boundary layer close to the surface and an isothermal outer flow. This outer flow is determined from equations (9) and (12) with $\theta = 0$. Together with the dimensionless boundary conditions

$$\eta = 0: \quad M = 0, \quad \frac{\partial M}{\partial \eta} = 0,$$

$$\eta \to \infty: \quad \frac{\partial M}{\partial \eta} = 0, \quad \frac{\partial M}{\partial \xi} + n\frac{M}{\xi} = 1, \tag{13}$$

these equations describe a Stokes' flow.

A solution has been proposed by Berry and Swain [7] for a two-dimensional flow around an infinite strip. Because this solution is logarithmically infinite far below the strip, the boundary condition

$$\frac{\partial M}{\partial \xi} = 1 \tag{14}$$

can only be satisfied for a finite η. The dimensionless stream function, M, was determined as

$$M = -\xi(\tanh x_1 - x_1), \tag{15}$$

where x_1 is one of the elliptic coordinates, which are related to the coordinates ξ and η by the transformation:

$$\xi = \cosh x_1 \times \cos x_2,$$
$$\eta = Pe^{1/4}\sinh x_1 \times \sin x_2. \tag{16}$$

The axisymmetric Stokes' flow around a circular plate is a limiting case of the flow around an ellipsoid. It was evaluated by Lamb [8]. The solution is described by a potential ϕ as

$$\phi = 1 - \frac{2}{\pi}\arctan\sqrt{\sigma}, \tag{17}$$

where σ is the positive root of the quadratic equation

$$\frac{\eta^2}{Pe^{1/2}\sigma} + \frac{\xi^2}{1+\sigma} = 1. \tag{18}$$

The velocity components can be determined from this potential as

$$\frac{\partial M}{\partial \eta} = -\frac{\eta}{Pe^{1/2}}\frac{\partial \phi}{\partial \xi},$$
$$\frac{\partial M}{\partial \xi} + \frac{M}{\xi} = \eta\frac{\partial \phi}{\partial \eta} - \phi + 1. \tag{19}$$

The solutions to both equations (15) and (19), can be expanded in series of ξ and η. In the lowest order, which still includes the finite size of the plate, one obtains

$$M = \left(m + \frac{2}{\pi}n\right)\frac{\eta^3}{3Pe^{3/4}}\left(\xi + \frac{3}{2}\xi^3\right), \tag{20}$$

with $m = n-1$. It will be proved below that this approach already describes a large part of the plate.

In order to describe the temperature boundary layer close to the surface, terms with $1/Pe^{1/2}$ can be neglected in equations (9), (11) and (12). Thus, the boundary layer flow is described by the equations

$$\frac{\partial M}{\partial \eta}\frac{\partial \theta}{\partial \xi} - \left(\frac{\partial M}{\partial \xi} + n\frac{M}{\xi}\right)\frac{\partial \theta}{\partial \eta} = \frac{1}{Pe^{3/4}}\frac{\partial^2 \theta}{\partial \eta^2}, \quad (21)$$

$$\frac{\partial^2 \omega}{\partial \eta^2} = -\frac{\partial \theta}{\partial \xi}, \quad (22)$$

$$\frac{\partial^2 M}{\partial \eta^2} = \frac{\omega}{A\,Pe^{3/4}}. \quad (23)$$

The dimensionless boundary conditions become

$$\eta = 0: \quad M = 0, \quad \frac{\partial M}{\partial \eta} = 0,$$

$$\theta = 1 \quad \text{for a specified surface temperature,}$$

$$\frac{\partial \theta}{\partial \eta} = -1 \quad \text{for a specified surface heat flux,}$$

$$\eta \to \infty: \quad \omega = 0, \quad \frac{\partial \omega}{\partial \eta} = 0, \quad \theta = 0. \quad (24)$$

In the case of high Prandtl numbers it cannot be a requirement that the horizontal velocity component dissappears outside the boundary layer.

The velocity components derived from the Stokes' flow are now inserted into the heat balance, equation (21). The temperature is expanded in a series of ξ as

$$\theta(\xi, \eta) = \theta_0(\eta) + \xi^2\theta_1(\eta). \quad (25)$$

It has been truncated to the same order as the stream function.

Now equation (21) can be grouped like powers of ξ and can be converted to a system of two linear ordinary differential equations. One obtains

$$\theta_0'' + \frac{1}{3}\left(m + \frac{4}{\pi}n\right)\eta^3\theta_0' = 0, \quad (26)$$

$$\theta_1'' + \frac{1}{3}\left(m + \frac{4}{\pi}n\right)\eta^3\theta_1' - \left(2m + \frac{4}{\pi}n\right)\eta^2\theta_1 = -\left(\frac{3}{2}m + \frac{4}{\pi}n\right)\eta^3\theta_0'. \quad (27)$$

Solutions of equation (26) are

$$\theta_0 = 1 - \frac{\int_0^\eta \exp\left[-\left(\frac{m}{12} + \frac{n}{3\pi}\right)\eta^4\right]\mathrm{d}\eta}{\int_0^\infty \exp\left[-\left(\frac{m}{12} + \frac{n}{3\pi}\right)\eta^4\right]\mathrm{d}\eta} \quad (28)$$

for a specified surface temperature, and

$$\theta_0 = \int_0^\infty \exp\left[-\left(\frac{m}{12} + \frac{n}{3\pi}\right)\eta^4\right]\mathrm{d}\eta - \int_0^\eta \exp\left[-\left(\frac{m}{12} + \frac{n}{3\pi}\right)\eta^4\right]\mathrm{d}\eta \quad (29)$$

for a specified surface heat flux.

These solutions are shown in Figs 2a and 3a. If θ_0 is inserted into equation (27), it can be solved numerically with a simple finite difference method. Results of θ_1 are shown in Figs 2b and 3b, respectively.

Next this temperature is inserted into the vorticity transport equation [equation (22)]. In this case, the temperature is derived with respect to ξ, so that only the temperature coefficient θ_1, which corresponds to the curvature of the isotherms, determines the vorticity profile. Now equation (22) can be integrated to yield a new vorticity function marked by an upper index I. One obtains

$$\omega^{\mathrm{I}} = 2\xi\omega_1(\eta), \quad (30)$$

where $\omega_1(\eta)$ is the vorticity profile, which is defined as

$$\omega_1(\eta) = -\int_\eta^\infty \int_\eta^\infty \theta_1(\eta)\,\mathrm{d}\eta^2. \quad (31)$$

These profiles are shown in Figs 2c and 3c, respectively.

If the new vorticity ω^{I} is inserted into equation (23), a new stream function M^{I} can be calculated. A first integration of equation (23) yields

$$\frac{\partial M^{\mathrm{I}}}{\partial \eta} = \frac{2\xi}{A\,Pe^{3/4}}U(\eta), \quad (32)$$

where $U(\eta)$ is defined as

$$U(\eta) = \int_0^\eta \omega_1(\eta)\,\mathrm{d}\eta. \quad (33)$$

$U(\eta)$ is the profile of the horizontal velocity component. It is shown in Figs 2d and 3d. A second integration yields

$$M^{\mathrm{I}} = \frac{2\xi}{A\,Pe^{3/4}}V(\eta), \quad (34)$$

where $V(\eta)$ is defined as

$$V(\eta) = \int_0^\eta U(\eta)\,\mathrm{d}\eta \quad (35)$$

which is the profile of the vertical velocity component. This function is shown in Figs 2e and 3e, respectively.

Now the outer expansion, described by equation (20), and the inner expansion, described by equation (32), can be matched. To determine the unknown relation between the Peclet number and the Grashof number, the total horizontal convective heat transport due to both stream functions, M and M^{I}, is set equally. We require that

$$\int_0^\infty \theta_0\frac{\partial M}{\partial \eta}\,\mathrm{d}\eta = \int_0^\infty \theta_0\frac{\partial M^{\mathrm{I}}}{\partial \eta}\,\mathrm{d}\eta. \quad (36)$$

Inserting equations (20) and (32) one obtains

$$\left(m + \frac{2}{\pi}n\right)\frac{\xi}{Pe^{3/4}}\int_0^\infty \eta^2\theta_0\,\mathrm{d}\eta = \frac{2\xi}{A\,Pe^{3/4}}\int_0^\infty \theta_0\,U(\eta)\,\mathrm{d}\eta. \quad (37)$$

This relation fixes the dimensionless group

$$A = \frac{Pe^{5/4}}{Gr\,Pr} \quad \text{or} \quad A = \frac{Pe^{3/2}}{Gr^*\,Pr}, \text{ respectively}$$

to a constant given in Table 1.

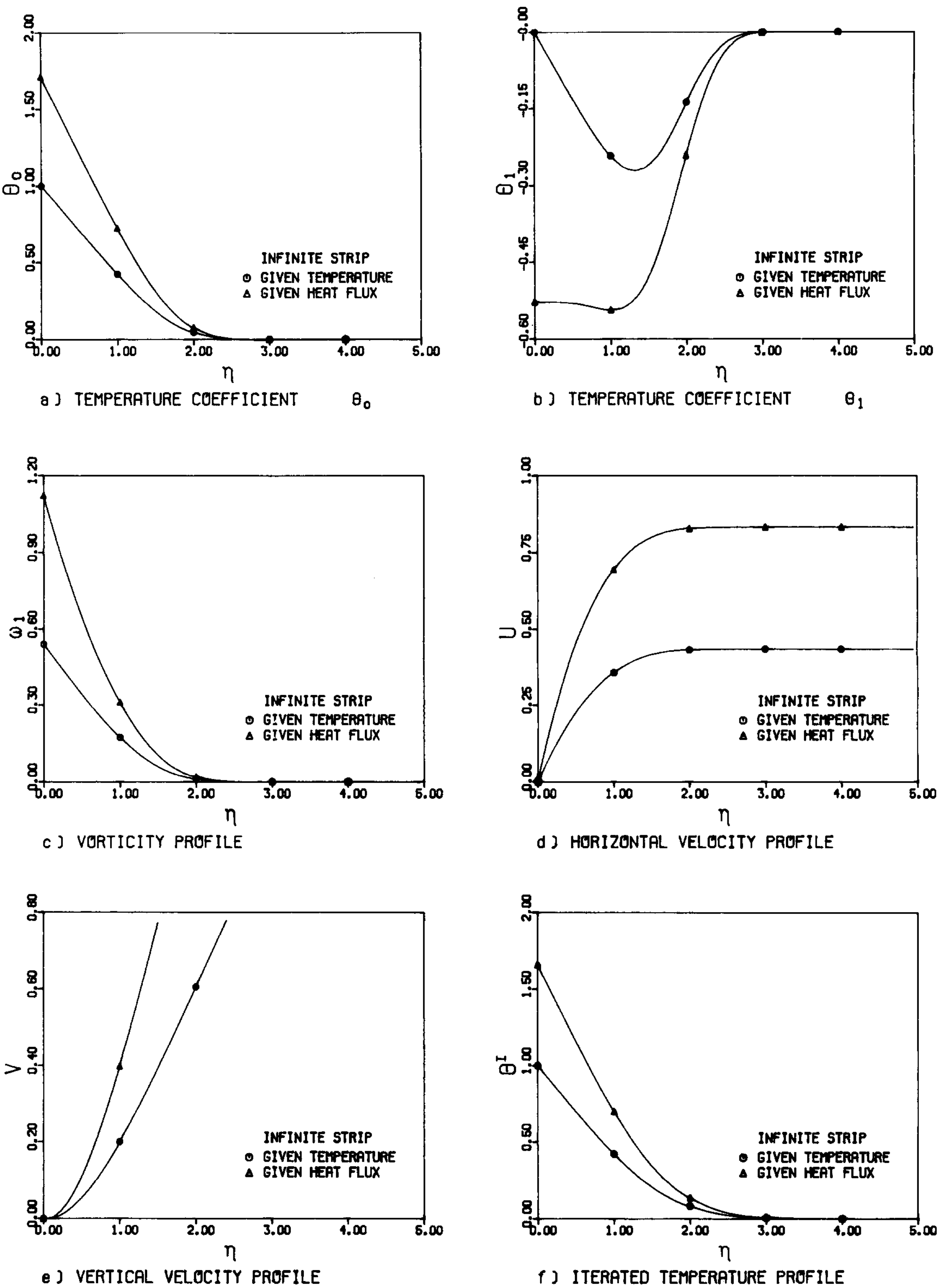

FIG. 2. Similarity solutions for high Prandtl numbers below an infinite strip.

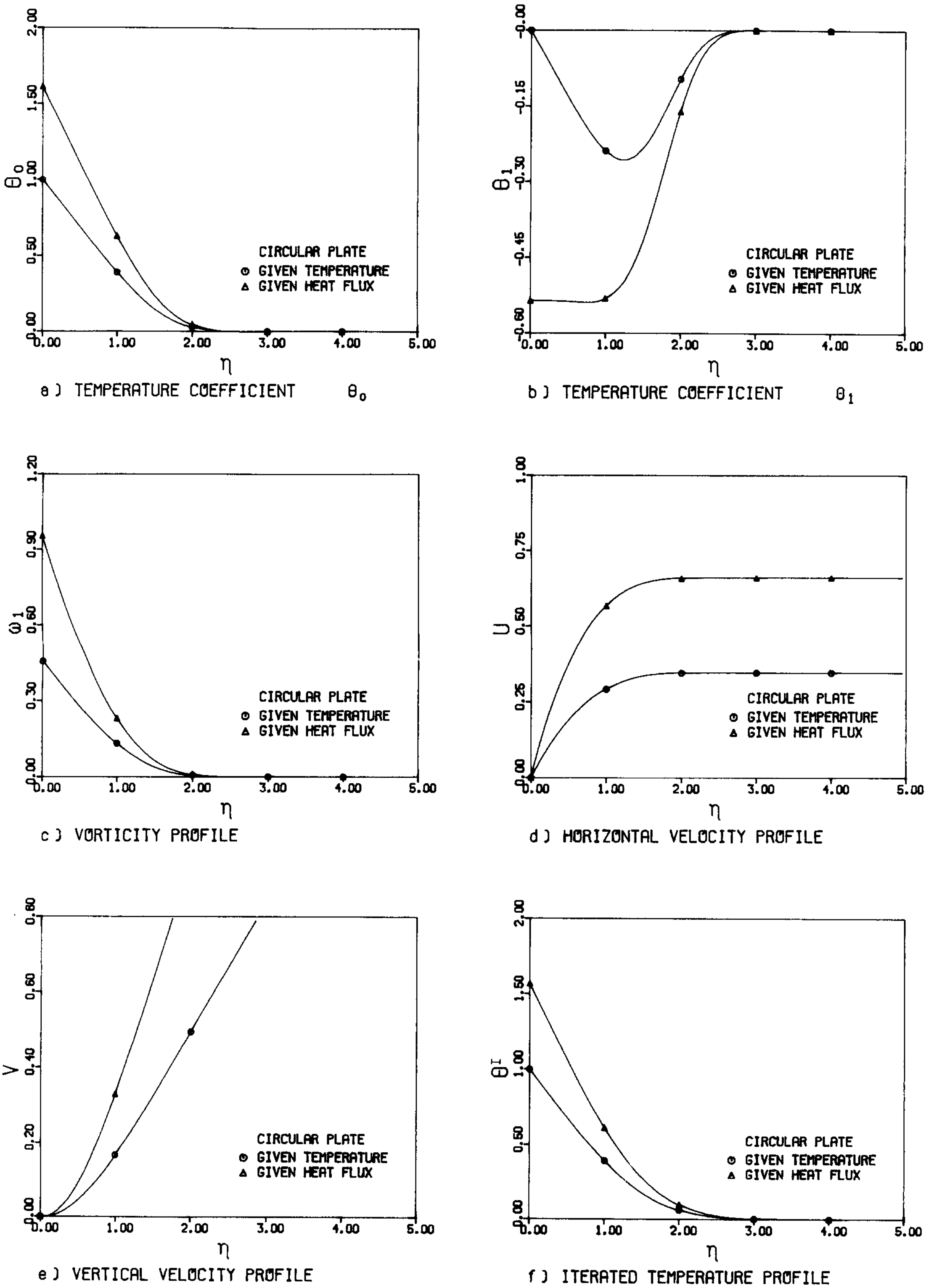

FIG. 3. Similarity solutions for high Prandtl numbers below a circular plate.

Table 1. Results for the dimensionless group A

A	Infinite strip	Circular plate
Specified surface temperature	0.703	0.991
Specified surface heat flux	1.384	1.950

Thus the Peclet number can be replaced by $(A\,Gr\,Pr)^{4/5}$ or by $(A\,Gr^*\,Pr)^{2/3}$, respectively. If this result is inserted into the solution of θ_0, equations (28) or (29), one obtains a correlation for the local Nusselt number in the vicinity of the stagnation point. This Nusselt number is defined as

$$Nu = \frac{q_w R}{\lambda(T_w - T_\infty)} = -Pe^{1/4}\frac{\left(\frac{\partial\theta}{\partial\eta}\right)_{\eta=0}}{\theta_{\eta=0}}. \quad (38)$$

Correlations are

$$Nu = 0.544(Gr\,Pr)^{1/5} \quad (39)$$

for an infinite strip with specified surface temperature,

$$Nu = 0.617(Gr^*\,Pr)^{1/6} \quad (40)$$

for an infinite strip with specified surface heat flux,

$$Nu = 0.619(Gr\,Pr)^{1/5} \quad (41)$$

for a circular plate with specified surface temperature and

$$Nu = 0.693(Gr^*\,Pr)^{1/6} \quad (42)$$

for a circular plate with specified surface heat flux.

To assure the accuracy of these correlations, the new stream function M^{I} is inserted again into the heat balance, equation (21). In the first order of ξ the new temperature θ^{I} can be determined from the ordinary differential equation

$$-2(1+n)V(\eta)\frac{\partial\theta^{\mathrm{I}}}{\partial\eta} = A\frac{\partial^2\theta^{\mathrm{I}}}{\partial\eta^2}. \quad (43)$$

It has been integrated numerically and the results are shown in Figs 2f and 3f, respectively. Local Nusselt numbers, which can be deduced from these results, differ by less than 2% from correlations (39)–(42).

Correlations for arbitrary Prandtl numbers

For a general correlation of heat transfer in fluids with arbitrary Prandtl numbers, the asymptote of low Prandtl numbers, derived in [6], and the asymptote of a high Prandtl number, which has been derived here, will be matched. As the Nusselt number is expected to vary uniformly between these limiting cases, an interpolation formula can be applied which has been proposed by Churchill and Usagi [9]. This formula interpolates the limiting heat transfer correlations as

$$\frac{1}{Nu^e(Pr)} = \frac{1}{Nu^e(Pr\to 0)} + \frac{1}{Nu^e(Pr\to\infty)}. \quad (44)$$

The exponent e has to be determined from experimental data for mean Prandtl numbers. The experimental results obtained by Aihara *et al.* [10], with an isothermal infinite strip in air, and the result of Faw and Dullforce [11], which had been measured with an isothermal circular plate in air, indicate an exponent of $e = 3$. These experiments have been considered as the most precise ones for this special application and it is assumed that the exponent ($e = 3$) can also be applied to plates with a specified surface heat flux.

Using the Rayleigh number Ra instead of Gr, Pr, and Ra^* instead of $Gr^*\,Pr$, the following correlations can be deduced for arbitrary Prandtl numbers. One obtains

$$\frac{Nu}{Ra^{1/5}} = \frac{0.571\,Pr^{1/5}}{[1+1.156\,Pr^{3/5}]^{1/3}} \quad (45)$$

for an infinite strip with specified surface temperature,

$$\frac{Nu}{Ra^{*1/6}} = \frac{0.643\,Pr^{1/6}}{[1+1.132\,Pr^{1/2}]^{1/3}} \quad (46)$$

for an infinite strip with specified surface heat flux,

$$\frac{Nu}{Ra^{1/5}} = \frac{0.705\,Pr^{1/5}}{[1+1.48\,Pr^{3/5}]^{1/3}} \quad (47)$$

for a circular plate with specified surface temperature, and

$$\frac{Nu}{Ra^{*1/6}} = \frac{0.776\,Pr^{1/6}}{[1+1.40\,Pr^{1/2}]^{1/3}} \quad (48)$$

for a circular plate with specified surface heat flux.

DISCUSSION

Using the results of asymptotically large and small Prandtl numbers, heat transfer correlations for arbitrary Prandtl numbers have been calculated for the region around the stagnation point in the centre of an infinite strip and of a circular plate. In Figs 4–7 these correlations are compared with experimental results and earlier theoretical approximations.

Singh *et al.* [1] were the first to apply an integral method of determining a heat transfer correlation for isothermal plates in a fluid with $Pr = 1$. For the special case of an isothermal infinite strip, Singh and Birkebak [2] extended this result to include arbitrary Prandtl numbers, which is shown in Fig. 4. These integral methods were based on empirical boundary layer profiles of temperature and velocity. Since only results in air had been available from Kraus [12] or Birkebak and Abdulkadir [13], these profiles had also been applied to fluids with arbitrary Prandtl numbers. Consequently, these predictions only agree with the general expression derived here for Prandtl numbers near unity. For higher Prandtl numbers, the velocity profile of air overpredicts the heat transfer, as the real velocity maximum is further outside the boundary layer than it was assumed in the integral method. For lower Prandtl numbers, the velocity close to the surface

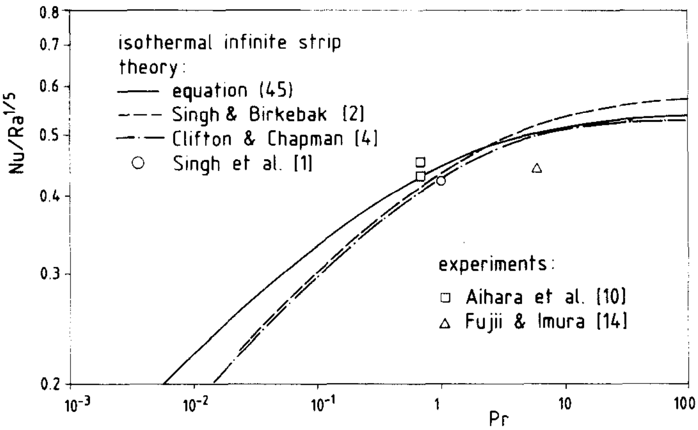

FIG. 4. Heat transfer correlations of an isothermal infinite strip.

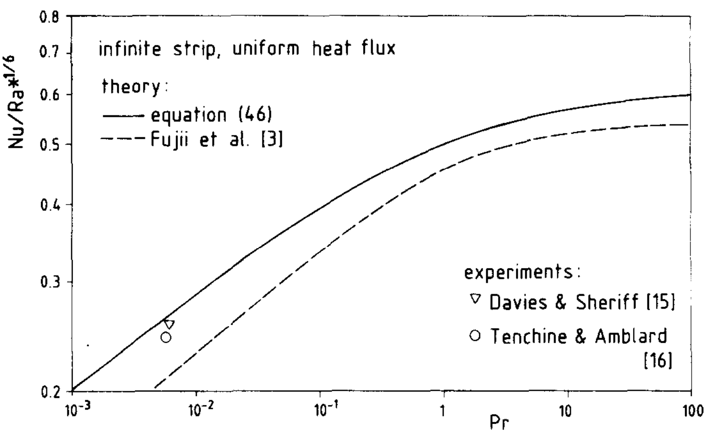

FIG. 5. Heat transfer correlations of a uniformly heated infinite strip.

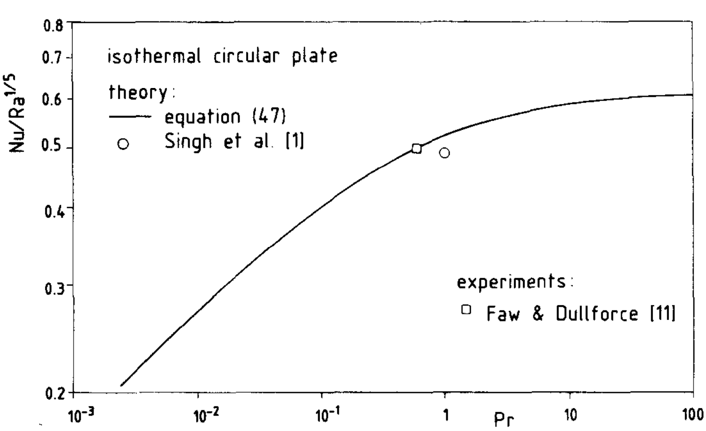

FIG. 6. Heat transfer correlations of an isothermal circular plate.

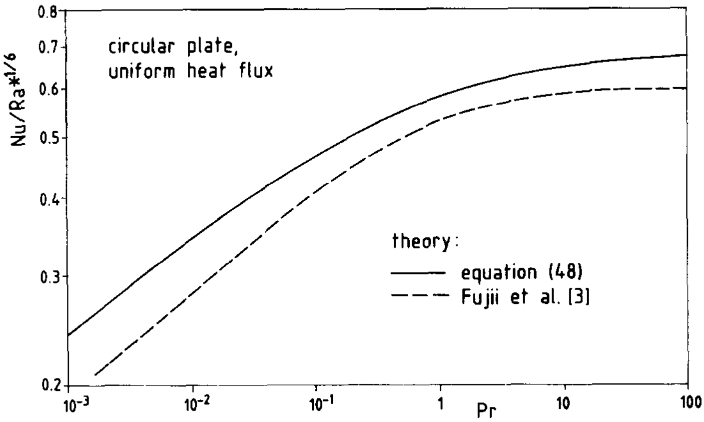

FIG. 7. Heat transfer correlations of a uniformly heated circular plate.

and hence the heat transfer correlation were underpredicted.

The experimental result of Fujii and Imura [14] which had been obtained in water is lower by more than 15% compared to results of other authors. It was probably a wrong interpretation by Fujii *et al.* [3] that this discrepancy could be due to the finite heat conductivity of the plate. For uniformly heated plates, they predicted a heat transfer correlation lower by 10–20% for all Prandtl numbers compared with the correlations derived here. This difference is demonstrated in Figs 5 and 7.

Recent results of Davies and Sheriff [15], and of Tenchine and Amblard [16], which have been measured in sodium, confirm the new correlations.

The infinite strip and the circular plate form a lower and upper boundary for heat transfer below rectangular plates with an arbitrary aspect ratio. As can be seen in Fig. 8 these boundaries differ by only 15%, so that simple interpolations between these limits are justified. An interpolation has already been proposed by Hatfield and Edwards [5] for the mean Nusselt number. Again the experimental results of Birkebak and Abdulkadir [13] and Restrepo and Glicksman [17] are in good accordance with these boundaries.

The similarity solutions which have been calculated here and in [6] were restricted to a region around the stagnation point where the local heat transfer is constant. It has already been demonstrated by Aihara *et al.* [10] that similarity solutions fail near the edges of the plate. To demonstrate the influence of the edges, the total heat transfer of the plate is compared with the local heat transfer at the stagnation point. In some experiments, a mean Nusselt number $\overline{Nu}$, averaged over the whole plate as well as the local Nusselt number, Nu, at the stagnation point were measured. Results of these experiments are shown in Fig. 9.* There the relative difference between the mean Nusselt number and the local Nusselt number at the stagnation point is plotted vs the Rayleigh number. This difference decreases with increasing Rayleigh numbers. For Rayleigh numbers higher than 10^7, it is lower than 10%. It can be deduced empirically from this plot that, with increasing Rayleigh numbers, the region of constant heat transfer extends over the whole plate. It should be mentioned explicitly here that all integral methods

*The experimental data of Faw and Dullforce [18] were extrapolated as $\overline{Nu}-Nu = 2\,(\overline{Nu}-Nu_l)$, in which Nu_l is a Nu-number averaged over a plate length.

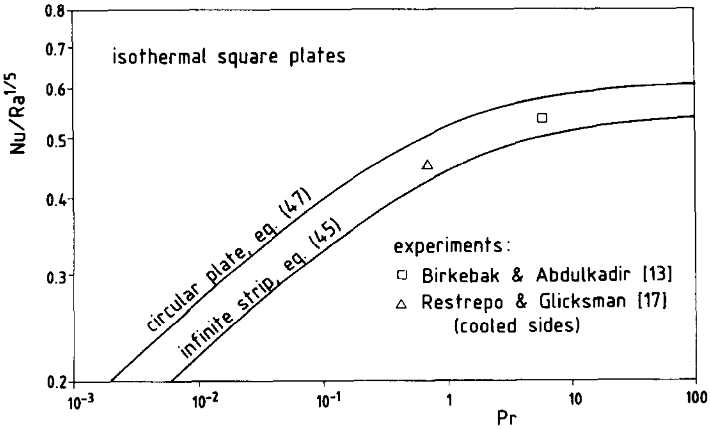

FIG. 8. Bounds for rectangular plates with an arbitrary aspect ratio.

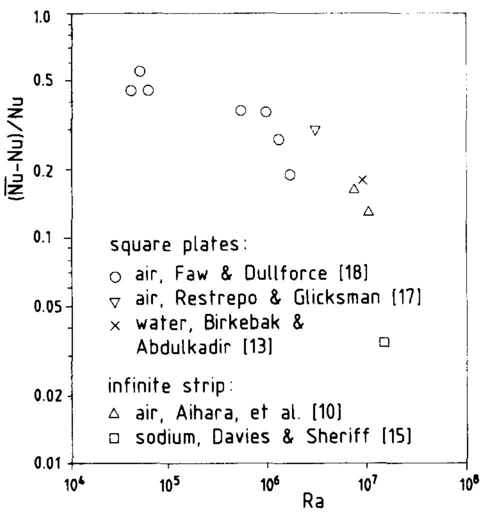

FIG. 9. Relative difference between the mean Nusselt number and the local Nusselt number near the stagnation point.

cited above, assumed a constant difference; consequently they do not describe this dependence on the Rayleigh number.

CONCLUSIONS

Local similarity solutions for high Prandtl numbers have been deduced with the method of matched asymptotic expansions. The iterative procedure takes into account the important effect of the flow outside the boundary layer. The results are independent of any empirical input.

Velocity and temperature profiles, which have been obtained for high Prandtl numbers, differ essentially from empirical profiles in air or water: with increasing Prandtl numbers the velocity maximum within the temperature boundary layer tends toward the outer flow. Therefore, these profiles are not independent of the Prandtl number, which is in contrast to assumptions of earlier integral methods.

From these similarity solutions, heat transfer correlations have been obtained for a region around the stagnation point. With increasing Rayleigh numbers this region extends over the whole plate.

An interpolation with heat transfer correlations for low Prandtl numbers, deduced in [6], yielded correlations for arbitrary Prandtl numbers. Nusselt numbers derived from these correlations differ by up to 20% from results obtained with integral methods. For uniformly heated plates they are predicted to be generally higher for all Prandtl numbers.

REFERENCES

1. S. N. Singh, R. C. Birkebak and R. M. Drake, Laminar free convection heat transfer from downward-facing horizontal surfaces of finite dimensions, *Prog. Heat Mass Transfer* **2**, 87–98 (1969).
2. S. N. Singh and R. C. Birkebak, Laminar free convection from a horizontal infinite strip facing downwards, *Z. Angew. Math. Phys.* **20**, 454–461 (1969).
3. T. Fujii, H. Honda and I. Morioka, A theoretical study of natural convection heat transfer from downward-facing horizontal surfaces with uniform heat flux, *Int. J. Heat Mass Transfer* **16**, 611–627 (1973).
4. J. V. Clifton and A. J. Chapman, Natural convection on a finite-size horizontal plate, *Int. J. Heat Mass Transfer* **12**, 1573–1584 (1969).
5. D. W. Hatfield and D. K. Edwards, Edge and aspect ratio effects on natural convection from the horizontal heated plate facing downwards, *Int. J. Heat Mass Transfer* **24**, 1019–1024 (1981).
6. T. Schulenberg, Natural convection heat transfer to liquid metals below downward facing horizontal surfaces, *Int. J. Heat Mass Transfer* **27**, 433–441 (1984).
7. A. Berry and L. M. Swain, On the steady motion of a cylinder through infinite viscous fluid, *Proc. R. Soc.* A 766–778 (1923).
8. H. Lamb, *Hydrodynamics*. Cambridge University Press, London (1975).
9. S. W. Churchill and R. Usagi, A general expression for the correlation of rates of transfer and other phenomena, *AIChE J.* **18**, 1121–1128, (1972).
10. T. Aihara, Y. Yamada and S. Endo, Free convection along the downward-facing surface of a heated horizontal plate, *Int. J. Heat Mass Transfer* **15**, 2535–2549 (1972).
11. R. E. Faw and T. A. Dullforce, Holographic interferometrie measurement of convective heat transport beneath a heated horizontal circular plate in air, *Int. J. Heat Mass Transfer* **25**, 1157–1166 (1982).
12. W. Kraus, Temperatur- und Geschwindigkeitsfeld bei freier Konvektion um eine waagerechte quadratische Platte, *Phys. Z.* **41**, 126–150 (1940).
13. R. C. Birkebak and A. Abdulkadir, Heat transfer by natural convection from the lower side of finite horizontal, heated surfaces. *Fourth International Heat Transfer Conference Paris*, Vol. 4, Paper NC2.2 (1970).
14. T. Fujii and H. Imura, Natural-convection heat transfer from a plate with arbitrary inclination, *Int. J. Heat Mass Transfer* **15**, 755–767 (1972).
15. N. W. Davies and N. Sheriff, An experimental investigation of natural convection heat transfer from downward facing surfaces in sodium for fast reactor internal core catchers, International Seminar of the ICHMT, Dubrovnik, 1–5 September 1980.
16. D. Tenchine and M. Amblard, Heat transfer by natural convection in sodium from downward facing surfaces, *Second International Topical Meeting on Nuclear Reactor Thermal Hydraulics*, Santa Barbara, U.S.A., 11–14 January, Vol. 2, pp. 1412–1417 (1983).
17. F. Restrepo and L. R. Glicksman, The effect of edge conditions on natural convection from a horizontal plate, *Int. J. Heat Mass Transfer* **17**, 135–142, (1974).
18. R. E. Faw and T. A. Dullforce, Holographic interferometry measurement of convective heat transport beneath a heated horizontal plate in air, *Int. J. Heat Mass Transfer* **24**, 859–869 (1981).

CONVECTION THERMIQUE NATURELLE SOUS UNE SURFACE HORIZONTALE TOURNEE VERS LE BAS

Résumé—La convection thermique laminaire et stationnaire sous une bande horizontale infinie et sous une plaque horizontale circulaire est déterminée analytiquement dans le cas des nombres de Prandtl élevés. La surface de la plaque est supposée soit isotherme, soit à flux uniforme. Cette convection est causée par la distribution non uniforme de température aux bords de la plaque. Ce problème est décrit par une équation elliptique qui n'était pas prise en compte dans les méthodes intégrales antérieures. Appliquant la méthode des développements asymptotiques, des solutions similaires sont déduites pour la région autour du point d'arrêt. Une interpolation avec le cas limite des faibles nombres de Prandtl fournit des formules pour le transfert thermique à des nombres de Prandtl arbitraires.

NATÜRLICHE KONVEKTION AN DER UNTERSEITE EINER EBENEN FLÄCHE

Zusammenfassung—Die laminare stationäre Konvektion an der Unterseite eines waagerechten, unendlich langen Streifens und einer waagerechten Kreisscheibe wird für den Grenzfall großer Prandtl-Zahlen analytisch untersucht. Die Oberfläche wird entweder als isotherm oder als gleichmäßig beheizt angenommen. Die Konvektionsströmung wird durch die ungleichmäßige Temperaturverteilung am Rande der Fläche verursacht. Daher muß dieses Problem durch eine elliptische Differentialgleichung beschrieben werden, was bei früheren Integralverfahren nicht berücksichtigt worden war. Durch Anwendung des angepaßten asymptotischen Näherungsverfahrens wurden Ähnlichkeitslösungen für die Umgebung des Staupunktes ermittelt. Darüberhinaus führt eine Interpolation mit dem Grenzfall kleiner Prandtl-Zahlen zu Wärmeübergangs-Korrelationen für beliebige Prandtl-Zahlen.

ТЕПЛОПЕРЕНОС ЕСТЕСТВЕННОЙ КОНВЕКЦИЕЙ ПОД ОБРАЩЕННЫМИ ВНИЗ ГОРИЗОНТАЛЬНЫМИ ПОВЕРХНОСТЯМИ

Аннотация—Ламинарная стационарная конвекция под горизонтальной узкой и горизонтальной круглой пластинами исследуется аналитически для предельного случая больших чисел Прандтля. Предполагается, что поверхность пластины является или изотермической, или равномерно нагреваемой. Конвекция вызывается неравномерным распределением температуры на краях пластин. Поэтому эту задачу следует описывать с помощью эллиптического дифференциального уравнения, что не учитывалось в ранее применявшихся интегральных методах. Методом сращиваемых асимптотических разложений получены решения подобия для области около точки торможения. Кроме того, посредством интерполяции на предельный случай малых чисел Прандтля получены зависимости для теплопереноса при произвольных числах Прандтля.